Desalination and Water Treatment
www.deswater.com

doi: 10.5004/dwt.2020.24948

178 (2020) 296–311
February

Application of artificial neural networks and response surface methodology for analysis of malachite green removal from aqueous solution using phosphoric acid–modified pumice powder: kinetic and isotherm studies

Noushin Osouleddini[a], Maryam Heydari[b], Mohammad Darvishmotevalli[c], Touba Khosravi[d,*]

[a]*Department of Chemistry, Ardabil Branch, Islamic Azad University, Ardabil, Iran, Tel. +989906866151; email: Osouleddini.n@gmail.com*
[b]*Department of Environmental Health Engineering, School of Public Health, Tehran University of Medical Sciences, Tehran, Iran, Tel. +989106806090; email:vida1heydari@gmail.com*
[c]*Student Research Committee, School of Health, Isfahan University of Medical Sciences, Isfahan, Iran, Tel. +989124256723; email: mohamad.darvish68@gmail.com*
[d]*Research Center for Environmental Determinants of Health, Health Institute, Kermanshah University of Medical Sciences, Kermanshah, Iran, Iran, Tel. +989189318647; email: touba_khosravi@yahoo.com*

Received 16 December 2018; Accepted 24 September 2019

ABSTRACT

The present study aimed at investigating phosphoric acid (1, 6 and 12 N)–modified pumice efficiency in removal of malachite green (MG) dye from aqueous solutions. The effects of different parameters such as pH (3–11), adsorbent dosage (0.2–1.4 g/L), contact time (15–75 min) and the dye initial concentration of 85 mg/L were analyzed. The obtained modified pumice was characterized using the Fourier transform infrared spectroscopy and scanning electron microscopy. Adsorption equilibrium data were analyzed using Langmuir, Freundlich, Temkin and Redlich–Peterson. The results illustrated that the data were following both Langmuir and Freundlich isotherms. Also, the phenol absorption was modeled using pseudo-first order, pseudo-second order, intraparticle diffusion and Elovich models. The best fit being observed with the pseudo-second-order kinetic model. Finally, the process modeling was carried out using response surface method and artificial neural networks.

Keywords: Adsorption; Pumice; Phosphoric acid; Malachite green; Response surface method; Artificial neural network

1. Introduction

Dye pollution in aquatic ecosystems is considered as one of the most frequent pollutants of the environment in recent years [1,2]. The colored wastewater is produced by various industries such as textiles, automotive, pharmaceutical, tanneries, cosmetics and healthcare. However, a large amount of these dyes are strongly persistent in biodegradation due to their complex structures. Naturally this may result in poisonous, carcinogenic and mutagenic solutions for humans and animals [3]. Such colored effluents are important, regarding esthetics. These reduce sunlight penetration through the water, disturb photosynthetic phenomena and the aquatic flora, as well as affect the aquatic organisms, the biological balance and the decomposition processes in receiving water [4]. Malachite Green (MG) is a cationic dye and one of the high consuming materials. It is utilized in various industries such as cotton, silk, paper, wool, leather, etc. It is also used in the fishing industries as antifungal and microbes to control parasites and fish diseases. The

* Corresponding author.

triphenylmethane dyes, such as the MG cause carcinogenic, genotoxic, mutagenic and abortion diseases due to their nitrogen contents specially in animals backbone [5]. Although using MG dyes have been banned in some countries, but they are also widely used in most parts of the world. This is because of their low costs, feasibility, high efficiency and deficiency of suitable alternative dyes [6,7]. Some researchers studied the removal of MG dye from aquatic environments by various natural materials such as timber waste, apple peel, *Annona squamosa* seed, pomegranate peel, scoria, etc. [8–11]. Among these materials, pumice is a more acceptable adsorbent due to its inexpensive and wide availability in different parts of the world [12]. Many researchers used pumice successfully to remove various environmental pollutants, including dyes, pesticides, phenolic compounds, heavy metals, etc., from aqueous solutions [12–15].

According to several advantages of pumice stone such as porous structure (about 85%), high specific surface area and its availability in Iran, this study aims at investigating the removal of the MG dye from aqueous solutions by modified pumice. Moreover, its hardness is high due to the great amounts of silica content (59%–72% of SiO_2) [5–7]. It could be stated that acids effected chemical composition, ion exchange and specific surface area of the pumice. The aim of this study is to evaluate the effects of phosphoric acid (1, 6 and 12 N) on pumice efficiency in removal of the MG dye from aquatic environments and also to determine the model, isotherm and kinetics of the reaction.

The common methods to optimize a multi-factorial system includes one factor at a time, which takes more time and does not show the effects of different options in ingredients [15,16]. So one of the most appropriate statistical methods to investigate the effects of one or more dependent and independent variable is response surface method (RSM) [17–21]. In the present work, the central composite design (CCD) for modeling and optimizing MG dye removal from aquatic environments by pumice has been investigated to evaluate the interactions between variables along with their direct impacts on the process [22]. As RSM is only suitable for quadratic approximations, interpretation of the impact of parameters is really difficult in adsorption due to the complexity of the reactions. Therefore, a promising alternative modeling approach such as artificial neural networks (ANN) is used in this study. The mathematical description of the phenomena in the process has not been required in the ANN model so the simulation of the complicated systems could be performed more efficiently.

2. Materials and methods

2.1. Preparation of adsorbate (MG), adsorbent and its modification

All chemical materials used in this study were purchased from the Merck Company (Germany). A specific amount of phosphoric acid was mixed with distilled water, and the phosphoric acid solutions with 1, 6 and 12 N were prepared and used for pumice modification. The hydrochloric acid and sodium hydroxide 1 M were used to adjust the pH of the solution. The Malachite green (MG) dye was purchased from the Merck Company with a catalog number of 105 – 20. And the stock solution (1,000 mg/L) of MG was prepared, and then the operating concentrations of stock solutions were prepared during the process. In the present study, the pumice stone as an adsorbent was collected from Qorveh, Kurdistan, Iran. At first, the pumice was washed thoroughly by de-ionized water to remove its impurities, and this was continued until the effluent's turbidity reached less than 1 NTU. Then 300 g of pumice stone was crushed and sieved with an effective size of 50#. The prepared powder was washed several times by de-ionized water and then it was dried in an oven at the temperature of 105°C for about 1 h. Then a specific amount of pumice powder was kept in phosphoric acid (1, 6 and 12 N) and placed on a shaker for 24 h. Finally, the modified pumice powder was washed several times by de-ionized water to remove residual phosphoric acid from the adsorbent and then dried at 105°C for 14 h [23].

2.2. Adsorbent characteristics

The chemical and physical properties of bare and modified adsorbent were characterized by Fourier transform infrared spectroscopy (FTIR), XRD and scanning electron microscopy (SEM). The FTIR was carried out using a spectrometer (WQF-510) with a resolution of 4 cm^{-1} in the range of 400–4,000 cm^{-1} with the KBr pellets technique. The chemical characteristics were determined by the XRD method (Shimadzu XRD-6000, Kyoto, Japan). The SEM (Philips XL30, Netherlands) technique was used for electron beam image of the adsorbent.

2.3. Experimental design (determining the sample size)

In this study, the DOE software [24] is used to design experiments (the required sample size). The design included 20 runs with 4 central points as shown in Table 1. The pH of 7 for discharging industrial effluent was recommended by the Iranian national standard (No: 2439). In experimental runs, the pH of 7, the absorbent dosage of 0.8 g/L, and the contact time of 45 min were considered. It should be noted that in all experimental runs, the initial concentration of MG dye was 85 mg/L.

2.4. Preparation of samples and adsorption study

MG is an azo dye with molecular formula $C_{23}H_{26}N_2CL$ (molecular weight of 364.5 g/mol; Table 2). The stock solution of 1,000 mg/L was prepared by dissolving 1 g of MG in 1,000 mL de-ionized water. For each analysis, run used the concentrated solution of 85 mg/L. The analysis of samples was carried out in a pH of 3, 5, 7,, 9 and 11, the contact time of 15, 30, 45, 60 and 75 min, adsorbent dosages of 0.2, 0.5, 0.8, 1.1 and 1.4 g/L with a mixing rate of 200 rpm.

The residual MG in sample was determined at different times. At first, 15 mL of the solution was centrifuged at 2,000 rpm for 15 min to separate the adsorbent, and then remaining the solute concentration was measured by a spectrophotometer (Cary 50 made by Perkin Elmer) at 665 nm [6]. All experiments were repeated three times to achieve acceptable results. Also, the calibration curve was calculated due to the absorbance rate and dye concentrations to prepare the standard solution.

Table 1
Used experimental range of variables

Variables	Range and level				
	−α (−1.5)	−1	0	1	+α (1.5)
Contact time, min	15	30	45	60	75
Adsorbent dosage, g/L	0.2	0.5	0.8	1.1	1.4
pH	3	5	7	9	11

Table 2
Characteristics and chemical structure of phosphoric acid and malachite green

Composition	Molecular weight	Chemical formula
Phosphoric acid	97.99	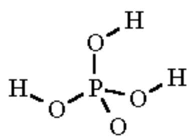
Malachite green	364.9	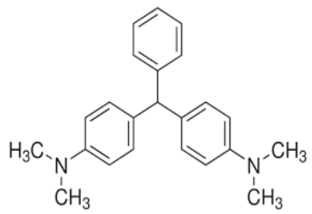

2.5. Adsorption isotherms study

The adsorption isotherms were used to evaluate the highest absorbance of the pollutants by the adsorbent. They could evaluate how of the adsorbent react regarding absorption materials, also they played an important role in the optimization of applying adsorbent.

In this study, the results were fitted well to Langmuir and Freundlich adsorption isotherms. All experiments were analyzed in five different adsorbent dosages (0.2, 0.5, 0.8, 1.1 and 1.4 g) with other parameters set constant (pH = 7, mixing rate of 200 rpm, 85 mg/L and contact time of 75 min). The amount of solute absorbed on pumice powder was calculated by the following equation [25]:

$$q_e = \frac{\left(C_0 - C_e\right)V}{m} \tag{1}$$

where q_e is the adsorption capacity at equilibrium (mg/g), C_0 and C_e are the initial and equilibrium concentrations of solute MG dye, respectively. (mg/L), V is the volume of solution (L) and M is the adsorbent weight (g).

2.5.1. Langmuir isotherm

The Langmuir isotherm was used based on monolayer adsorption on the adsorbent surface, which contained a limited and uniform number of adsorption sites. The Langmuir isotherm derivative presented a homogeneous absorption, so that each molecule had enthalpies and constant activation energy [26].

The linear form of the Langmuir isotherm could be calculated as follows:

$$\frac{1}{q_e} = \frac{1}{Q_m} + \frac{1}{bQ_mC_e} \tag{2}$$

where C_e and b are equilibrium concentration (mg/L) and equilibrium constant (mg/L), respectively; and q_m is the maximum absorption capacity (mg/g).

One of the most important Langmuir isotherm parameters is dimensionless constant R_L (separation factor), which is used by Webber and Chakkravorti to calculate the shape of the Langmuir isotherm [27]. R_L equation is defined as follows:

$$R_L = \frac{1}{\left(1 + bC_0\right)} \tag{3}$$

where R_L is the separation factor, C_0 is the initial concentration (mg/L) and b is the Langmuir constant.

Absorption process could be determined using R_L parameters

Factor R_L	Type of absorption process
$R_L > 1$	Undesirable
$R_L = 1$	Linear
$0 < R_L < 1$	Desirable
$R_L = 0$	Irreversible

2.5.2. Freundlich isotherm

In this study, the Freundlich isotherm was used to describe the non-ideal and reversible absorption for multilayer adsorption on heterogeneous adsorbent sites with unequal and non-uniform energy. And it is not limited to single-layer absorption [28].

The linear form of Freundlich isotherm could be represented as follows:

$$q_e = \log K_f + \frac{1}{n}\log C_e \tag{4}$$

where q_e is the amount of solute adsorbed (mg/g), C_e is equilibrium concentration (mg/L), K_f and n are constants related to the absorption capacity ((mg/g) (g/L) (l/n)) and intensity of absorption, respectively [29].

2.5.3. Temkin isotherm

The Temkin isotherm could be calculated by the following equation [30]:

$$q_e = \frac{RT}{b_t}\ln K_t C_e \tag{5}$$

where R is ideal gas constant (8.314 J/mol K), T is absolute temperature (K) and b_t is the Temkin equation constant (J/mol).

2.5.4. Redlich–Peterson isotherm

The Redlich–Peterson isotherm could be calculated by the following equation [31]:

$$q_e = \frac{k_{\mathrm{RP}} C_e}{1 + \alpha C_e \beta} \tag{6}$$

where K_{RP} is the Redlich–Peterson isotherm constant, α and β are the Redlich–Peterson isotherm constants.

2.6. Reaction kinetic study

To investigate the MG dye absorption processes and the absorption rate control, the reaction kinetic was used. Constancy of the reaction kinetic was calculated by the use of the following Lagergren pseudo-first-order and Hu pseudo-second order equations [32].

To obtain the reaction kinetics, the mixing time and other parameters were considered constant (the dye absorbance rate at different mixing times of 15, 30, 45, 60 and 75 min, and constant dosage of 0.8 g and 200 rpm).

2.6.1. Pseudo-first order kinetic

The linear form of the first-order kinetic equation was shown as follows [33]:

$$\log\left(1 - \frac{q_t}{q_e}\right) = -\frac{K_1}{2.302} t \tag{7}$$

q_t and q_e are the amounts of adsorbed dye at time t, and equilibrium (mg/g), k_1 is the pseudo-first-order kinetic rate constant (min^{-1}).

2.6.2. Pseudo-second order kinetics

The linear pseudo-second-order model can be revealed as follows [33]:

$$\frac{t}{q_t} = \frac{1}{h} + \frac{1}{q_e} t \tag{8}$$

$$h = k q_e^2 \tag{9}$$

where h is the primary absorption rate when $t \to 0$ (mg g^{-1}min^{-1}), and k is the pseudo-second-order kinetic adsorption constant (g mg^{-1} min^{-1}).

2.6.3. Intraparticle diffusion kinetics

The intraparticle diffusion model can be revealed as the following equation [34]:

$$q_t = k_{\mathrm{id}} t^{\frac{1}{2}} \tag{10}$$

where k_{id} is the rate constant for intra-particle diffusion models and t is time (min).

2.6.4. Elovich kinetics

The Elovich model can be revealed as the following equation [35]:

$$q_t = \frac{1}{d}\ln(cd) + \frac{1}{d}\ln t \tag{11}$$

where c is the initial adsorption rate (mg/(g min)) and d is the Elovich constant (g/mg).

2.7. Artificial neural network

An artificial neural network is a flexible mathematical structure that can identify complex nonlinear relationships between input and output data sets [36,37]. In this study, a multilayer feed forward neural network with a hidden layer was trained by the back-propagation gradient-descendent algorithm. The experimental points were determined using the CCD method (Table 5) to train and test the model. These experimental points were divided into three sets of trainings; validation and testing included 70%, 20% and 20% of the data, respectively. Training data were used to update the weight and biases using the Levenberg Marquardt algorithm, and testing data were used to assess the trained network generalization capability. Also, the error of validation data was monitored during training to eschew over fitting [38]. The network used in this study consists of three input nodes (contact time, adsorbent dosage and pH) in the first layer and an output node (dye removal) in the third layer. For the neurons in the input and output layers, linear function (purelin) and hidden layer, hyperbolic tangent sigmoid function (tansig) was applied [39]. The number of neurons in the hidden layer was employed as a model design parameter due to their significant impact on network performance. Therefore, to determine the optimal number of neurons in this layer, different topologies were investigated and the mean square error (MSE) in each topology was calculated using the following equation [40]:

$$\mathrm{MSE} = \frac{\sum_{i=1}^{N}\left(y_{i,\mathrm{pred}} - y_{i,\exp}\right)^2}{N} \tag{12}$$

where $y_{i,\mathrm{pred}}$ and $y_{i,\exp}$ are the predicted and experimental values of the response, respectively, and N illustrates the number of data points.

To avoid random correlation due to random measurements of weights and biases, each topology was repeated 10 times [41].

To compare the ANN and RSM models, the following performance indexes were computed: R^2, R^2_{adj}, RMSE, MAE, AAD (Eqs. (13)–(17)) [42].

$$R^2 = 1 - \left(\frac{\sum_{i=1}^{N}\left(y_{i,\mathrm{pred}} - y_{i,\exp}\right)^2}{\sum_{i=1}^{N}\left(y_{i,\exp} - y_{i,m}\right)^2}\right) \tag{13}$$

$$R^2_{\text{adj.}} = 1 - \left(\left(1 - R^2\right) \frac{N-1}{N-K-1} \right) \tag{14}$$

$$\text{RMSE} = \left(\frac{\sum_{i=1}^{N} \left(y_{i,\text{pred}} - y_{i,\text{exp}} \right)^2}{N} \right)^{\frac{1}{2}} \tag{15}$$

$$\text{MAE} = \frac{1}{N} \left(\sum_{I=1}^{N} \left| y_{i,\text{pred}} - y_{i,\text{exp}} \right| \right) \tag{16}$$

$$\text{AAD} = \frac{1}{N} \left(\sum_{I=1}^{N} \frac{\left| y_{i,\text{pred}} - y_{i,\text{exp}} \right|}{y_{i,\text{exp}}} \right) \times 100 \tag{17}$$

where K is the number of input variables and $y_{i,m}$ is the average of experimental response.

3. Results and discussion

3.1. Characterization of adsorbent

The results of FTIR are shown in Fig. 1, in modifying the adsorbent with phosphoric acid, proton penetrates the adsorbent structure and attacks the O–H bonds of the adsorbent. Thus, it changes the absorption capacity of the O–H bands and octagonal cations. The results also showed that the peak was excited in 1,000 to 3,500 cm^{-1} bands due to the effect of the acid proton on the O–H. Whereas, the high-pitched peaks could be observed in 788 to 1,066 cm^{-1} bands, which are related to the Si–O–Si. Also, the bands of 525, 690 and 998 cm^{-1} are linked to the Si–O–Al [43]. It also indicated that the content of aluminum in the pumice structure is decreased in terms of increased phosphoric acid normality. Therefore, the 3,608 and 3,780 cm^{-1} peak band, related to AlO–H and Si–OH–Al groups, are decreased with increasing the acid normality [44]. On the other hand, a bandwidth in 3,550 cm^{-1} will be formed with increasing the acid normality, which is related to SiO–H groups [45]. Table 3 shows the results of the XRF analysis. As it could be observed, the aluminum content of pumice decreased from 19.6% in raw pumice to 14.4% in modified pumice in terms of increased normality of phosphoric acid (12 N). These findings confirmed the results of the FTIR, because the pumice-related peaks have also been reduced due to decreased its aluminum content. Fig. 2 shows the SEM results. The pumice has an irregular structure with porous surfaces, which create a lot of absorption sites on pumice. The pumice modified by the phosphoric acid in three investigated concentrations shows a lot of similarities. Although the surface of the pumice is large due to more porosity, increasing the acid normality is not destroying the pumice structure [46].

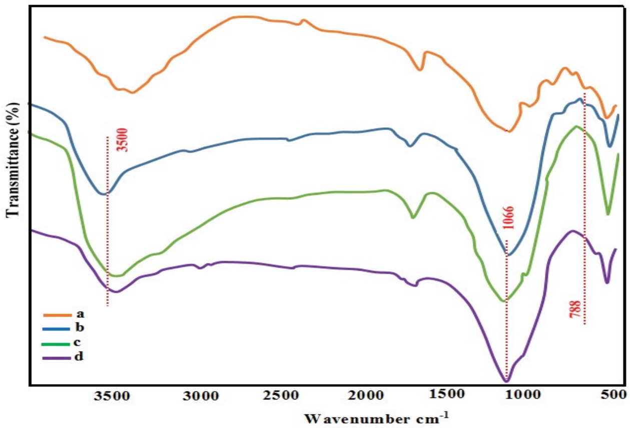

Fig. 1. Absorbent FTIR, (a) raw scoria, (b) modified 1 N phosphoric acid-pumice, (c) modified 6 N phosphoric acid-pumice, and (d) modified 12 N phosphoric acid-pumice.

3.2. Validity of the RSM model

To determine the correlation between the predicted and actual results, the ANOVA analysis test was used. The ANOVA test was performed to measure the significance and adequacy of the model, and the results are presented in Table 4. The statistical analysis of the results also shows that the actual removal rate of malachite dye is near to predicted value. On the other hand, the *F*-value represents the ratio of the squared model for the ratio of the squared errors,

Table 3
Raw scoria and modified (1, 6 and 12 N) phosphoric acid-pumice

Raw pumice	%	Modified (1 N) phosphoric acid-pumice	%	Modified (6 N) phosphoric acid-pumice	%	Modified (12 N) phosphoric acid-pumice	%
SiO_2	48.79	SiO_2	50	SiO_2	52.36	SiO_2	56.25
Al_2O_3	19.6	Al_2O_3	17.86	Al_2O_3	15.7	Al_2O_3	14.4
K_2O	4.4	K_2O	2.14	K_2O	1.89	K_2O	1.55
Fe_2O_3	9.1	Fe_2O_3	7.68	Fe_2O_3	6.95	Fe_2O_3	6.88
CaO	7.9	CaO	7.59	CaO	6.68	CaO	6.23
MgO	8.05	MgO	7.03	MgO	6.47	MgO	6.27
P_2O_5	1	P_2O_5	6.53	P_2O_5	8.4	P_2O_5	7.25
TiO_2	1	TiO_2	0.95	TiO_2	0.87	TiO_2	0.8
etc.	0.16	etc.	0.22	etc.	0.68	etc.	0.37

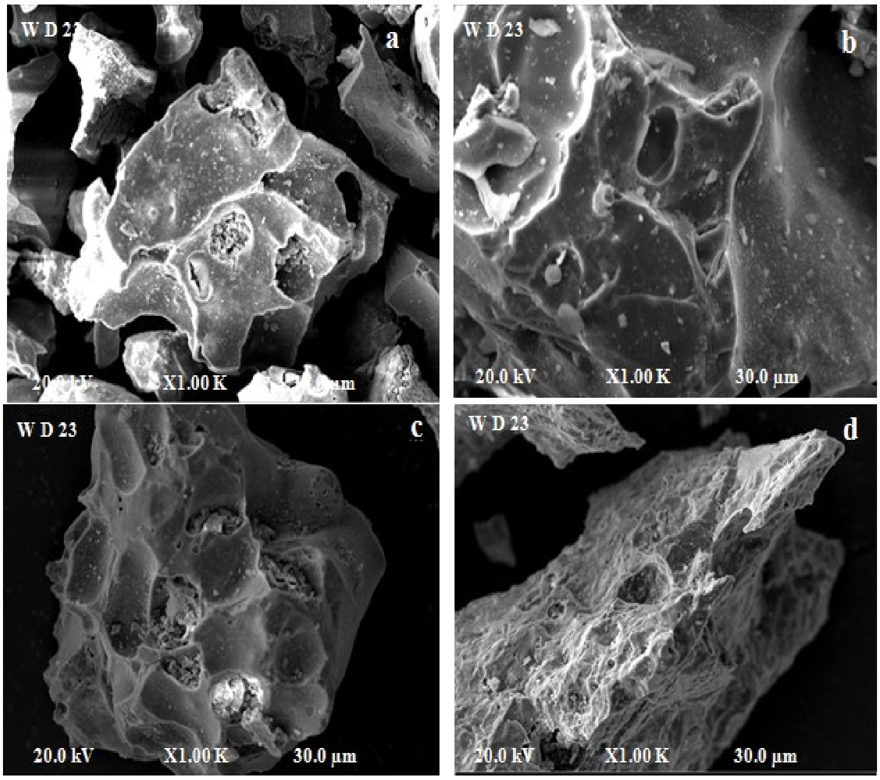

Fig. 2. SEM image of absorbent (a) raw scoria, (b) acid phosphoric-modified pumice (1 N), (c) phosphoric acid-modified pumice (6 N), and (d) phosphoric acid-modified pumice (12 N).

Table 4
Malachite dye removal model by phosphoric acid-modified pumice (1, 6 and 12 N) and parameters validity of tests

Phosphoric acid	Modified equations with significant terms	Type of model	F value	Prob > F	Mean	SD	R^2	Adj. R^2	Pred. R^2	AP	PRESS	PLF
1 N	Removal (%) = +61.32 + 4.48A + 13.81B + 20.71C	Linear	59.36	0.001>	61.32	5.53	0.9176	0.9021	0.8599	31.563	830.26	0.056
6 N	Removal(%) = +65.74 + 4.08A + 13.42B + 20.19C	Linear	44.6	0.001>	65.74	5.74	0.9070	0.8896	0.8235	29.38	999.48	0.114
12 N	Removal (%) = +70.02 + 4.63A + 12.98B + 20.13C	Linear	40.17	0.001>	70.02	6.48	0.8828	0.8608	0.7710	26.04	1,312.44	0.071

SD: standard deviation, R^2: determination coefficient, Adj. R^2: Adjusted R^2, Pred. R^2: Predicted R^2, AP: adequate precision, PRESS: predicted residual error sum of squares, PLF: probability for lack of fit.

which indicates a high value of the F-value, low error rate and high compliance of the model [47]. The F-value and p-value were used to control the level of the interaction and significance of the independent variables. The high F-value shows the high effect of the intended parameter. Although the p-value is lower and the F-value is higher, the coefficient associated with that factor or the independent variable is more impressive and important. The results indicated that all the parameters mentioned above are suitable for the proposed models (Prob > F and PLF < 0.05, and AP > 4). Therefore, this issue implies the reliability of the obtained models to predict the amount of dye removal. The results also showed that the contrast between the actual and predicted values of MG dye removal by the modified pumice decreases with increasing the normality of using acid in adsorbent modification. As, with increasing the normality, the dispersion of points, which represents the percentage of actual removal rate on the line, shows more predicted values.

3.3. Effect of variables on the response

Table 5 shows the average percentage of actual and predicted malachite dye removal rate by the phosphoric acid-modified scoria (1, 6 and 12 N). As the results showed,

Table 5
Mean of actual and predicted removal percentage of Malachite Green dye by the modified pumice with different concentrations of phosphoric acid (1, 6 and 12 N)

	Variables			Responses (Removal of dye %)											
	Factor1	Factor2	Factor3	Phosphoric acid											
				1 N			6 N			12 N			Raw pumice		
Run	*A*: Contact time, min	*B*: Adsorbent dosage, g/L	*C*: pH	Actual	RSM predicted	ANN predicted	Actual	RSM predicted	ANN predicted	Actual	RM predicted	ANN predicted	Actual	RSM predicted	ANN predicted
1	15	0.2	3	22.5	22.3	21.93	24.0	22.2	24.00	28.8	32.3	28.66	20.5	16.70	20.50
2	75	0.2	3	32.2	31.3	29.62	35.5	34.6	35.50	39.4	41.5	41.20	22.2	24.40	22.67
3	45	0.8	7	63.5	61.3	65.29	42.1	69.4	41.76	72.2	70.0	74.89	54.0	51.60	54.00
4	45	0.8	7	66.5	61.3	65.29	67.1	69.4	68.76	74.2	70.0	74.89	54.0	51.60	54.00
5	45	0.8	7	68.5	61.3	65.29	71.1	69.4	68.76	76.2	70.0	74.89	54.0	51.60	54.00
6	75	1.4	11	94.7	100.3	90.01	95.9	97.6	95.9	99.8	107.8	96.51	82.5	86.50	87.91
7	75	1.4	3	53.5	58.9	59.89	55.6	55.7	55.6	59.2	67.5	59.14	45.5	49.50	45.50
8	45	0.8	7	60.5	61.3	65.29	68.1	69.4	68.76	73.2	70.0	74.89	54.0	51.60	54.00
9	15	0.2	11	57.5	63.7	56.69	61.1	61.1	61.10	62.9	72.5	63.61	47.6	53.70	47.67
10	45	0.8	7	61.5	61.3	65.29	69.1	69.4	68.76	74.2	70.0	74.89	54.0	51.60	54.00
11	75	0.2	11	68.2	72.7	67.02	71.5	71.8	71.80	75.4	81.8	74.21	65.8	61.40	65.80
12	45	0.8	9	77.7	71.7	78.30	81.9	75.9	85.96	86.6	80.1	87.08	66.1	60.80	66.10
13	60	0.8	7	66.1	63.6	71.58	73.4	70.6	73.40	79.4	72.3	74.01	57.4	53.50	57.40
14	15	1.4	3	43.7	49.9	48.79	50.4	50.1	50.40	52.2	58.2	52.23	34.7	41.80	29.06
15	45	1.1	7	80.3	68.2	76.41	83.1	78.2	83.10	85.9	76.5	88.20	70.6	57.90	70.59
16	30	0.8	7	57.2	59.1	50.69	64.4	66.6	64.4	67.3	67.7	70.46	46.8	49.60	46.80
17	45	0.8	5	45.2	51.0	45.24	50.3	55.7	48.44	54.3	60.0	55.85	38.6	42.30	40.07
18	15	1.4	11	91.4	91.4	92.24	92.8	93.7	91.23	96.4	98.5	96.49	78.2	78.80	78.19
19	45	0.5	7	51.3	54.4	47.85	60.5	64.8	60.5	67.5	63.5	63.34	41.8	45.30	41.80

the removal of MG dye by the phosphoric acid-modified scoria has significantly increased rather than raw pumice in parallel conditions. The maximum removal efficiency was obtained by the phosphoric acid (12 N), (6 N) and (1 N)-modified pumice. It indicated that the ability of chemical changes in the adsorbent for removal of alumina and silica increases with increasing the acidity due to breaking the molecular bands. Also, the intensity of replacing the hydrogen ions with metals (iron, potassium and titanium) in the adsorbent structure was increased; therefore, the efficiency of adsorbent will be increased consequently, because it causes some changes in pumice structure including a significant increase in the surface area, pores diameter and three-dimensional deformation. So, this change in structure increases the absorbing dye due to increase in the surface area and absorption sites [48]. These results are confirming other researchers' studies. For example, the study of Ajemba [48] on the nitric acid-modified bentonite showed that the adsorption of silica increased but the content of cations (Al^{+3}, Fe^{+2} and Mg^{+2}) was decreased significantly in terms of increasing the acid concentration. The reason could be due to the fact that the cations, mentioned above, are eight-sided plates that are entering the solution during modifying the adsorbent with acid. While the silica remains in the adsorbent content in result of its four square structure. Increasing the ratio of Si/[Al^{+3}, Fe^{+2}, Mg^{+2}] increases the free space in adsorbed crystalline tissue, consequently increases the absorption capacity of bentonite. Also, in modifying the adsorbent with nitric acid, the proton cannot fill the vacant cations due to proton acid ion exchange with Na^{+}, K^{+}, Ca^{+2}, Al^{+3} and Mg^{+2}, so the created free space causes an increase in the absorption capacity of the adsorbent. As well in nitric acid modified-adsorbent, Mg^{+2} cation is separated easily from the adsorbent rather than Al^{+3}, Fe^{+2} cations [49]. Guo et al. [50] study indicated that nitric acid increased oxygen groups on activated carbon adsorbent, thus increased the absorption of positively charged pollutants.

Figs. 3 and 4 show the comparison among the effects of contact time, adsorbent dose and pH on the efficiency of malachite dye removal by modified pumice. The results indicated that the dye removal rate increases by increasing contact time, adsorbent dose and pH. The highest effect was related to pH, adsorbent dose and contact time, respectively [51]. Findings also indicated that the line slope of the pH (*C*) was greater than the line slopes of absorbent dose (*B*), and contact time (*A*). Therefore, it confirmed the efficiency of parameter in dye removal process (Figs. 5 and 6). However, with concentration increase, the trend of using acid in modifying pumice, and the slopes are close to each other. It could be due to the removal of dyes increased in terms of increasing the acid normality for modifying the adsorbent. Also, higher affectivity of the pH rather than other factors (absorbent dose and contact time) could be due to the higher affectivity of pH on the physical and chemical properties of adsorbent and adsorbate, because the adsorbent surface is negatively charged with increased pH. Regarding this, the MG is a cationic dye with two nitrogen atoms and methyl agents [52]. Therefore, in alkaline environments, where the charge level of adsorbent is more, dye adsorption rate increases due to electrostatic gravity [53]. Also, the color of malachite changes more chemically for pH more than 9, so its adsorption is increased [54]. Moreover, the dye absorption decreased with pH decrease, it could be due to creating electrostatic repulsion in an acidic environment in terms of producing the proton ion (H^+). All in all, the absorption of cationic dye decreased. Furthermore, according to it, the dominant combination of pumice is SiO_2, and this combination is converted to Si^{+3} with decreasing the pH, which also causes electrostatic repulsion and thus reduces the absorption of the cationic dye. The dye slight absorption in an acidic environment was due to the dye penetration in the adsorbent pores. As well, high removal efficiency by acid-modified pumice in the acidic condition is more than bare pumice. Although, pumice modification with acid causes in increasing the positive charge on the adsorbent surface. It is more likely that the cationic absorption should be decreased due to electrostatic repulsion, because pumice modification causes an increase in adsorbent surface and pore volume, which could increase the adsorbent efficiency of acid-modified pumice more than raw pumice despite increasing the electrostatic refraction [52]. Other studies also revealed that the removal of MG dye by wood waste and removal of cationic dye by mango peel are both increased [51]. This study showed that the maximum removal rate of MG dye by activated carbon was observed in pH = 7 within pH 3 to 7. The absorbent surface is negative in pH close to alkaline, so it causes increasing the absorption of the malachite dye. But in acidic pHs, the charge level is positive due to overcoming the hydrogen ion, so the electro-static repulsion reduces the absorption of the cationic dye. Also, this study showed that for pHs less than 4 the adsorbent surface charge was more positive and for pH of 4 to 6 the adsorbent surface was heterogeneous and a combination of

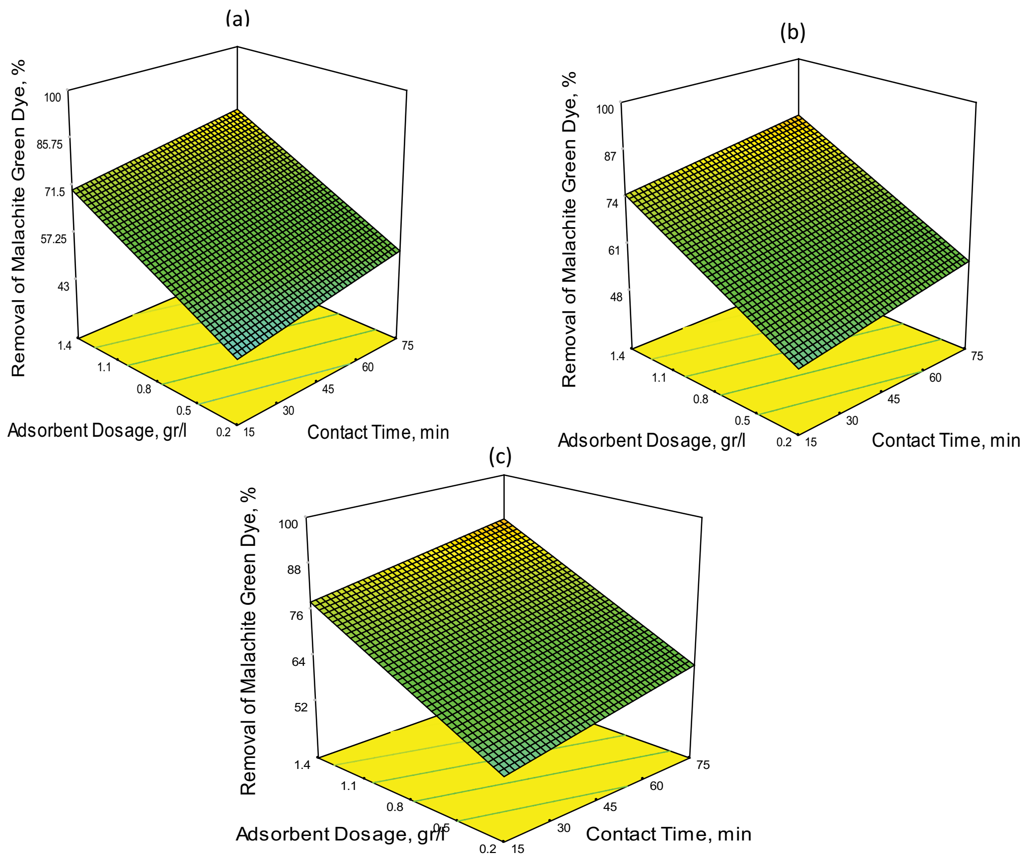

Fig. 3. Effect of contact time and absorbent dose at pH = 7 on the phosphoric acid-modified pumice acid (a): N, (b): 6 N, and (c): 12 N.

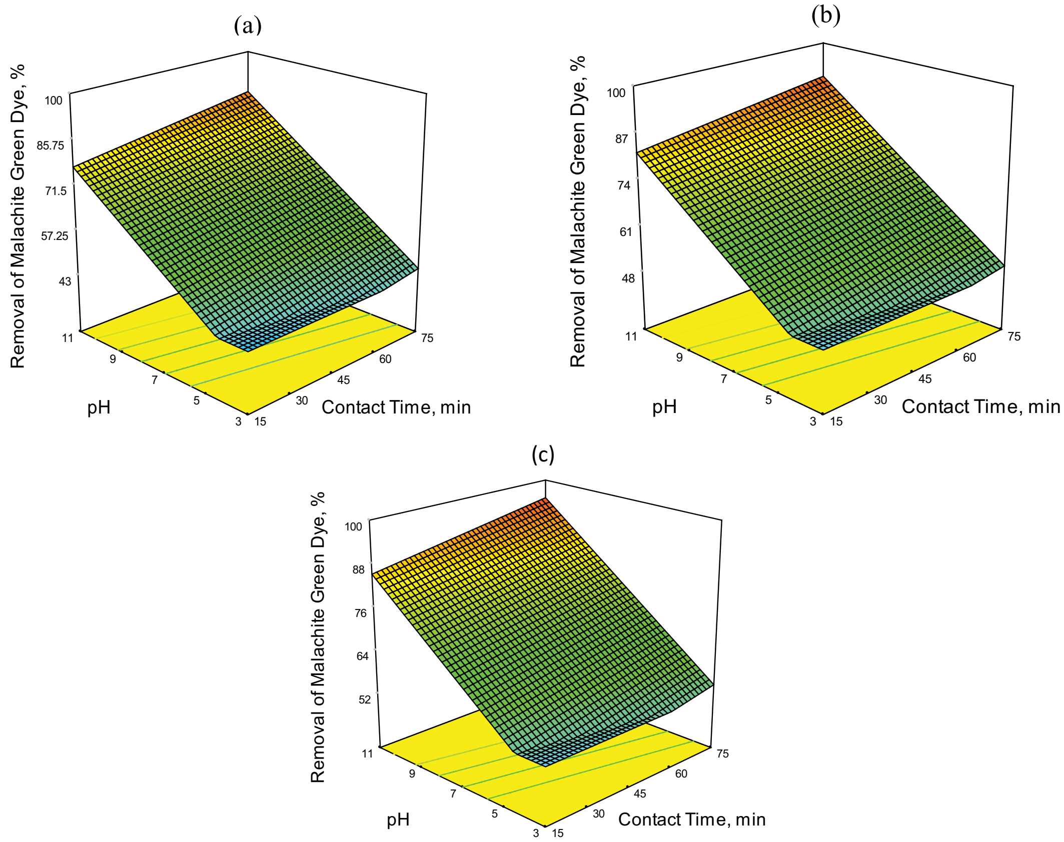

Fig. 4. Effect of contact time, pH and absorbance dose in removal of malachite dye on the phosphoric acid-modified pumice (a): N, (b): 6 N, and (c): 12 N.

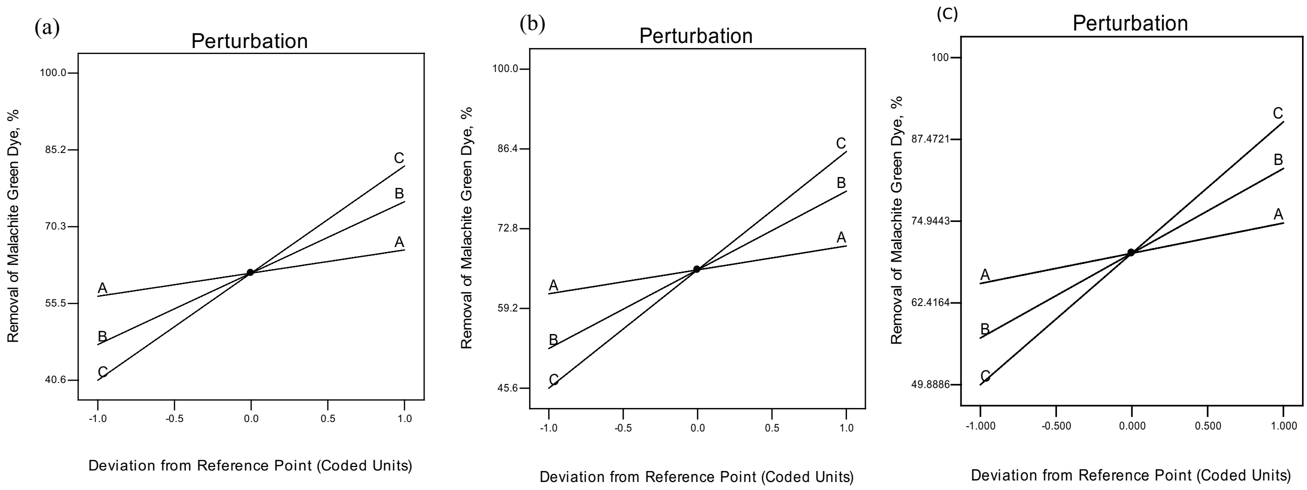

Fig. 5. Effect of absorbent dosage, contact time and pH parameters in the removal of malachite dye by the phosphoric acid-modified pumice (a): N, (b): 6 N, and (c): 12 N.

a negative and positive charge. But for pHs more than 6, the adsorbent surface was negatively charged due to hydroxyl. The results also showed that the removal rate of more than 50% occurred at the first 30 min and then decreased with increasing absorption time. The high absorption of dye at the initial contact time was reported at pH = 7 due to the negative charge on the adsorbent surface [55]. The results also showed that the optimum area for removal of more than 75% by the phosphoric acid (12 N)-modified pumice was higher than 6 N and this one was more than 1 N (Fig. 7).

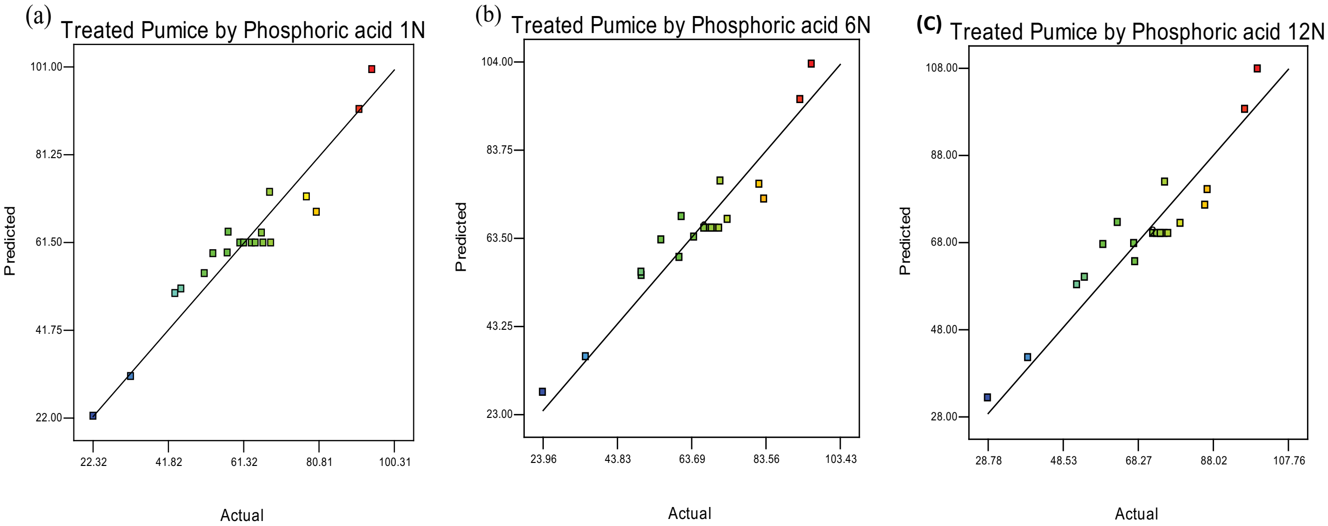

Fig. 6. Confrontation between actual and predicted value of the malachite dye removal by phosphoric acid-modified pumice (a): 1 N, (b): 6 N, and (c): 12 N.

3.4. Adsorption kinetics and isotherm

The adsorption isotherms investigation showed that the dye absorption fitted well with both the Langmuir and Freundlich isotherms. The separation coefficient (R_L) is the most important parameter in the Langmuir isotherm adsorption, which defines the adsorbent capability in separating and removing absorbents. The results showed that the maximum dye absorption capacity was increased with increased acid normality. So that Q_m for phosphoric acid (1 and 12 N)-modified pumice increased from 4.54 to 5.55 mg/g, which indicates an increase in the pumice adsorption sites with increasing the acid normality (Table 6). Also, in this study the Langmuir isotherm shows that the R_L of adsorbent is located in the optimal range (0–10). In other words, the acid-modified pumice is an appropriate adsorbent to remove the dye. These results are inconsistent with the results of Moraci and Calabrò [56]. The Freundlich isotherm study also showed that the maximum absorption coefficient (K_f) by the phosphoric acid-modified pumice forms were related to 1 N > 6 N > 12 N, respectively. It indicated that the adsorption sites increased with increased concentration of acid and its effect on the adsorbent structure increases. It can be stated that the acid causes some changes in the pumice structure, including a significant increase in pumice surface area, an increase in the diameter of the pore size and its three-dimensional deformation. Therefore, these structural changes cause an increase in the absorption sites and consequently increase the absorption of dye [57]. Also, the results showed that the absorption rate ($1/n$) calculated for all acid-modified pumice forms was in an optimal range (0–1). However, with increasing the normalization, the $1/n$ rate decreases. This indicated that modifying pumice with different concentrations of acid, different absorbent sites are available for dye adsorption, and hence with increasing the acid normality the absorption rate increases. Because in the Freundlich isotherm, the $1/n$ value represented the interaction between adsorbent and absorbent, and as $1/n$ tends to zero, that interaction is stronger and more powerful [58]. But Temkin and Redlich–Peterson isotherms cannot describe the data in different acid concentrations (Table 6).

The adsorption kinetic reactions on pumice showed that the adsorption process follows the pseudo-second order kinetic model for all absorbent forms. The results of other researcher's study on the removal of various cationic dyes with different adsorbents, showed that the adsorption data followed the pseudo-second order kinetics [57–62]. Obeying the pseudo-second order models imply that the adsorption process depends on the absorbent concentration, as

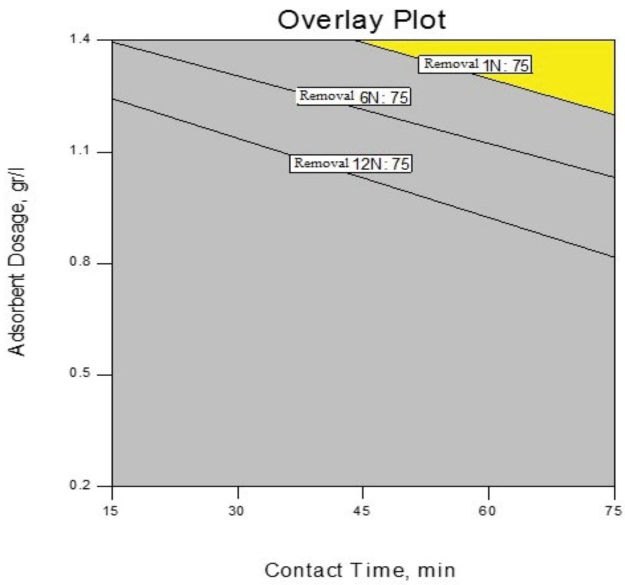

Fig. 7. Optimum area of removal efficiency more than 75% for phosphoric acid (1, 6 and 12 N)-modified pumice.

Table 6
Calculation of the constants of different isotherms and kinetic equations

Langmuir	Acid normality	Q_m (mg/g)	b (L/mg)	R_L	R^2
	1	4.54	0.076	0.134	0.904
	6	5.05	0.061	0.161	0.992
	12	5.55	0.107	0.098	0.99
Freundlich	Acid normality	K_f (mg/g)	$1/n$	R^2	
	1	0.8	0.401	0.902	
	6	0.74	0.461	0.99	
	12	1.08	0.374	0.971	
Temkin	Acid normality	K_t	b_t	R^2	
	1	0.18	0.17	0.257	
	6	0.24	0.21	0.229	
	12	0.42	0.54	0.212	
6	Acid normality	K_{RP}	α	R^2	
	1	2.33	0.090	0.261	
	6	1.69	0.141	0.301	
	12	1.59	0.120	0.300	
Pseudo-first order	Acid normality	K_1 (min^{-1})	R^2		
	1	0.03	0.947		
	6	0.0322	0.928		
	12	0.034	0.936		
Pseudo-second order	Acid normality	K_2 (g mg^{-1} min^{-1})	R^2		
	1	0.0173	0.961		
	6	0.0164	0.959		
	12	0.946	0.0177		
Intraparticle diffusion	Acid normality	k_{id}	R^2		
	1	0.0344	0.541		
	6	0.0360	0.562		
	12	0.0224	0.571		
Elovich	Acid normality	c	R^2		
	1	0.0079	0.441		
	6	0.0104	0.379		
	12	0.0082	0.270		

the pseudo-second-order equation is generally based on the adsorption capacity [63,64]. Also, in the case of kinetics, pseudo-first order, intraparticle diffusion and Elovich cannot describe the data in different acid concentrations (Table 6).

3.5. ANN model

In this study, the optimal ANN topology had three inputs, a hidden layer with six neurons and an output layer (1–6-3). The number of neurons in the hidden layer was selected by training different ANN topologies and selecting the optimal based on the maximization of R^2 and minimizing MSE. The values of R^2 and MSE for modified pumice with phosphoric acid with various concentrations (1, 6 and 12 N) and raw pumice are shown in Table 7. High R^2 values for optimal ANN topology confirmed the appropriation of this method for predicting the repeatability of experimental data. In Figs. 8–11, the predicted data are plotted against the experimental results for the training, validation, testing, and all data sets. These figures illustrate the appropriate fit between the experimental data and the predicted data by the ANN model.

3.6. Comparison of RSM and ANN models

Table 8 shows the comparative performance between ANN and RSM models. According to this table, the RMSE, MAE and AAD values for the ANN model are less than RSM. On the other hand, the R^2 values of ANN are higher than RSM, which suggests that experimental data can be predicted more accurately with the ANN model. Additionally, the R^2_{adj} values are closer to R^2 in the ANN model, which is related to the better ANN performance. Therefore, these results confirm that the ANN model is more reliable for predicting this nonlinear system.

Table 7
Relationship between number of neurons in hidden layer with MSE and R^2

Number of neuron s in hidden layer	1 N		6 N		12 N		Raw pumice	
	MSE	R^2	MSE	R^2	MSE	R^2	MSE	R^2
2	69.572	0.804	66.912	0.804	51.840	0.887	13.845	0.968
3	50.367	0.830	45.198	0.875	29.909	0.936	5.345	0.980
4	29.866	0.882	14.961	0.955	16.990	0.951	5.230	0.983
5	51.036	0.903	3.356	0.989	8.042	0.977	5.053	0.980
6	14.402	0.957	1.825	0.995	5.152	0.983	3.101	0.990
7	19.421	0.948	18.241	0.911	6.656	0.978	11.985	0.950
8	24.078	0.929	39.564	0.876	10.995	0.964	15.225	0.947
9	36.893	0.918	57.775	0.838	42.902	0.905	21.501	0.926
10	58.599	0.874	77.563	0.823	61.748	0.861	49.984	0.835

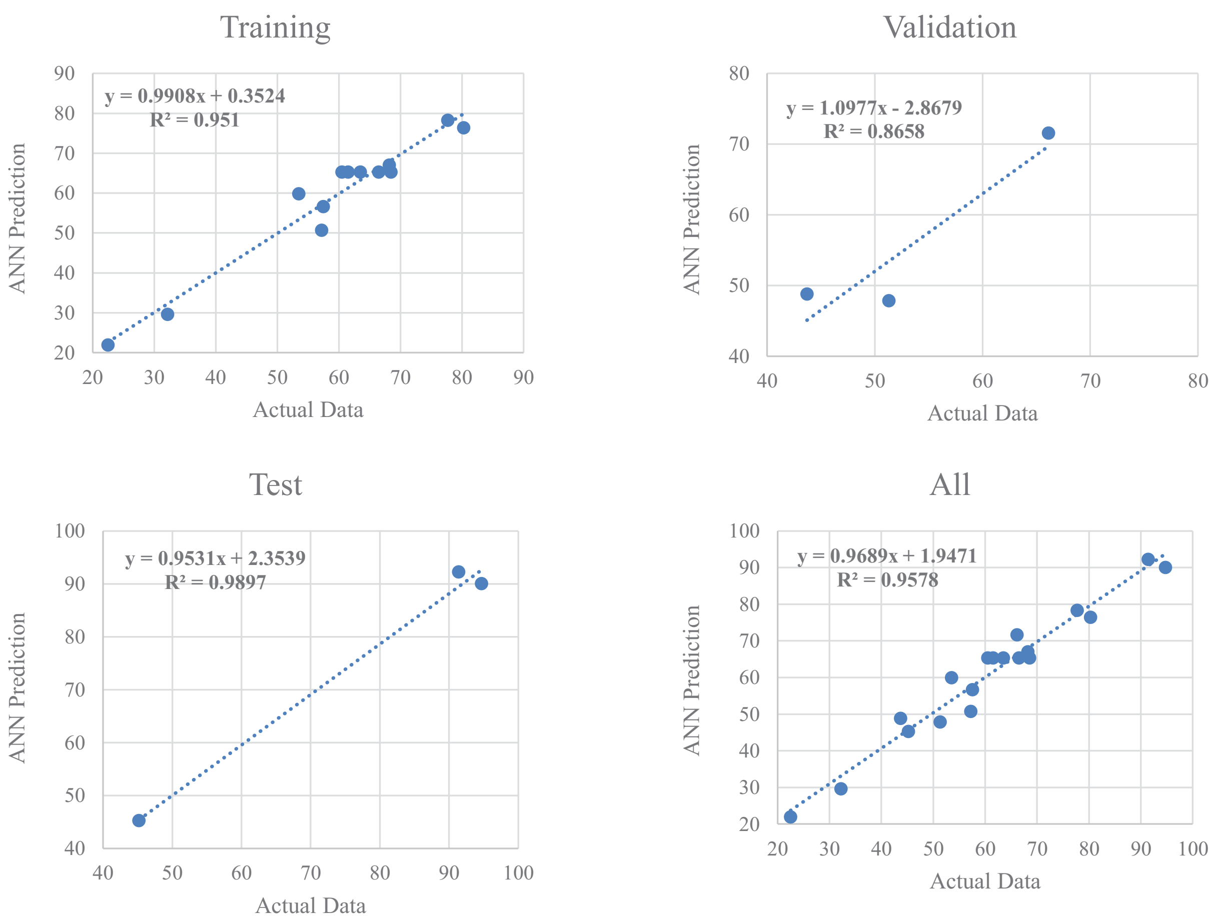

Fig. 8. Scatter plot of the ANN predicted vs. experimental data of MG dye removal by modified pumice with 1 N phosphoric acid.

4. Conclusion

According to the obtained results, the phosphoric acid improved the removal rate of the MG dye through chemical changes (especially the ratio of silica to alumina) in adsorbent structure and also increased the specific surface area. Absorption efficiency increased with increased dose, contact time and pH. To understand the mechanisms of the considered process better, the equilibrium adsorption isotherms and kinetic models were applied. The results indicated that the data have obeyed both Langmuir and Freundlich isotherms. Based on the correlation coefficient,

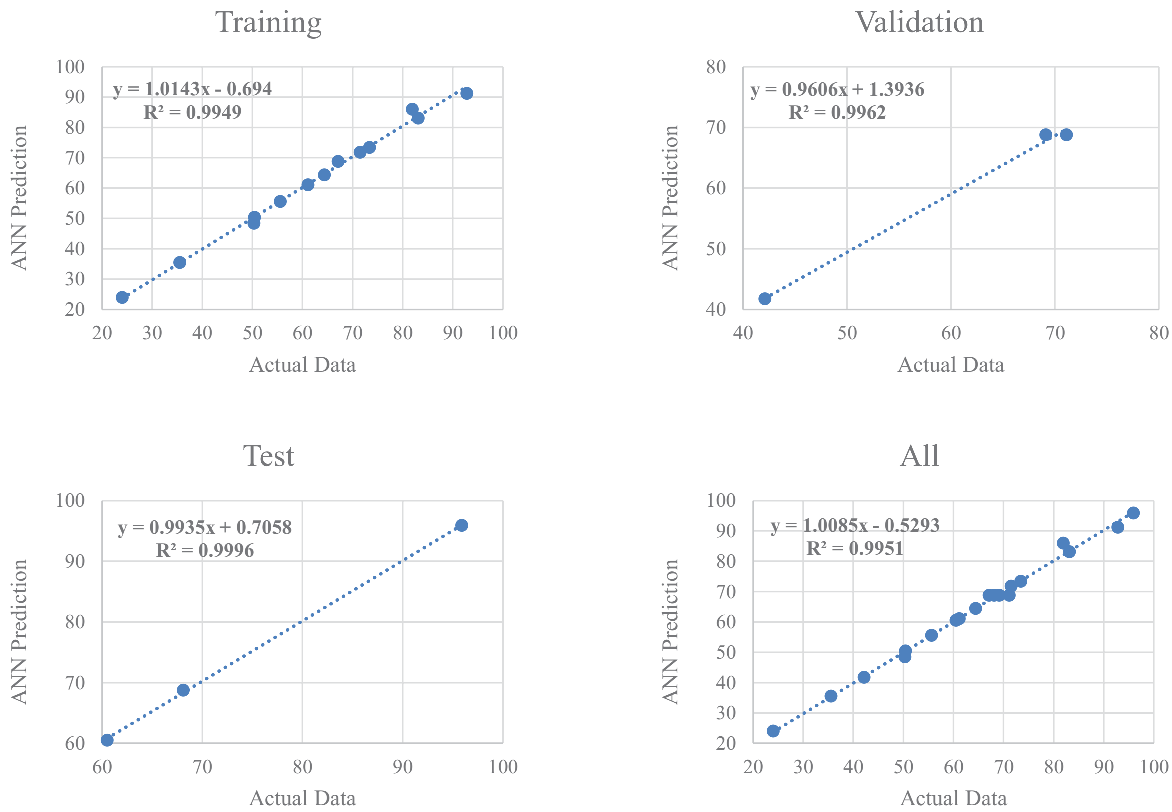

Fig. 9. Scatter plot of the ANN predicted vs. experimental data of MG dye removal by modified pumice with 6 N phosphoric acid.

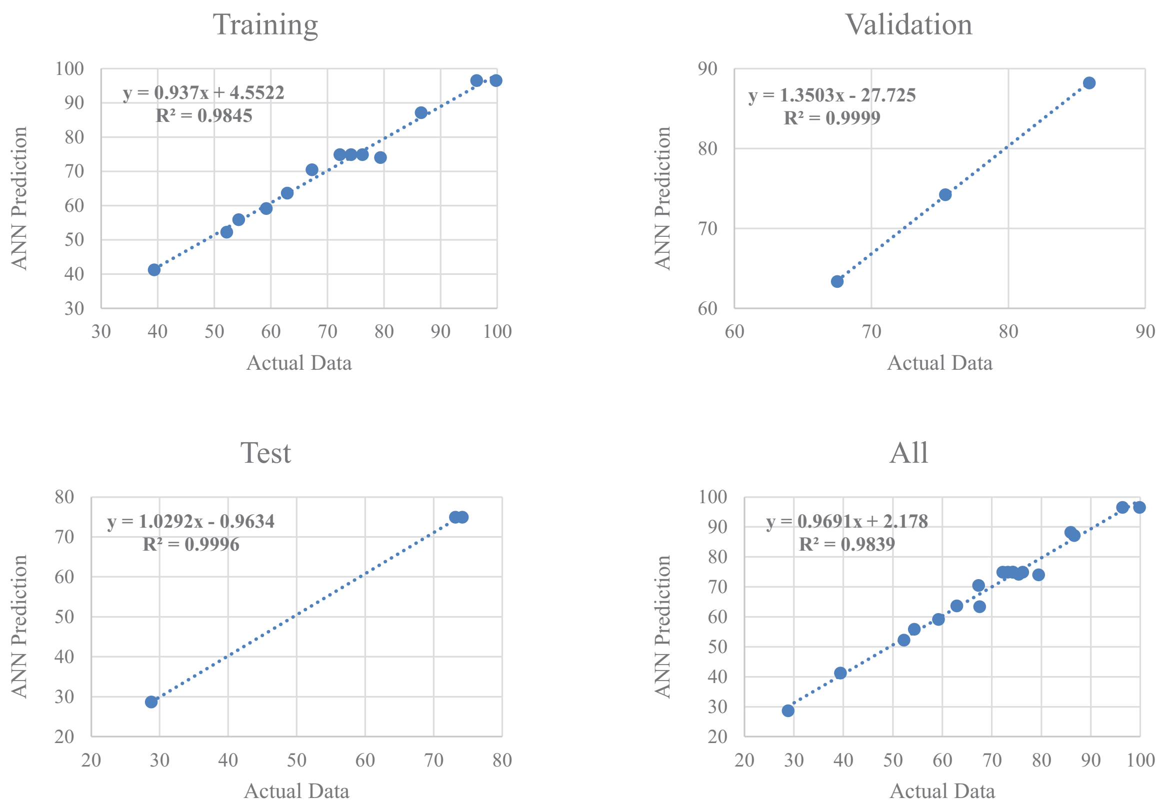

Fig. 10. Scatter plot of the ANN predicted vs. experimental data of MG dye removal by modified pumice with 12 N phosphoric acid.

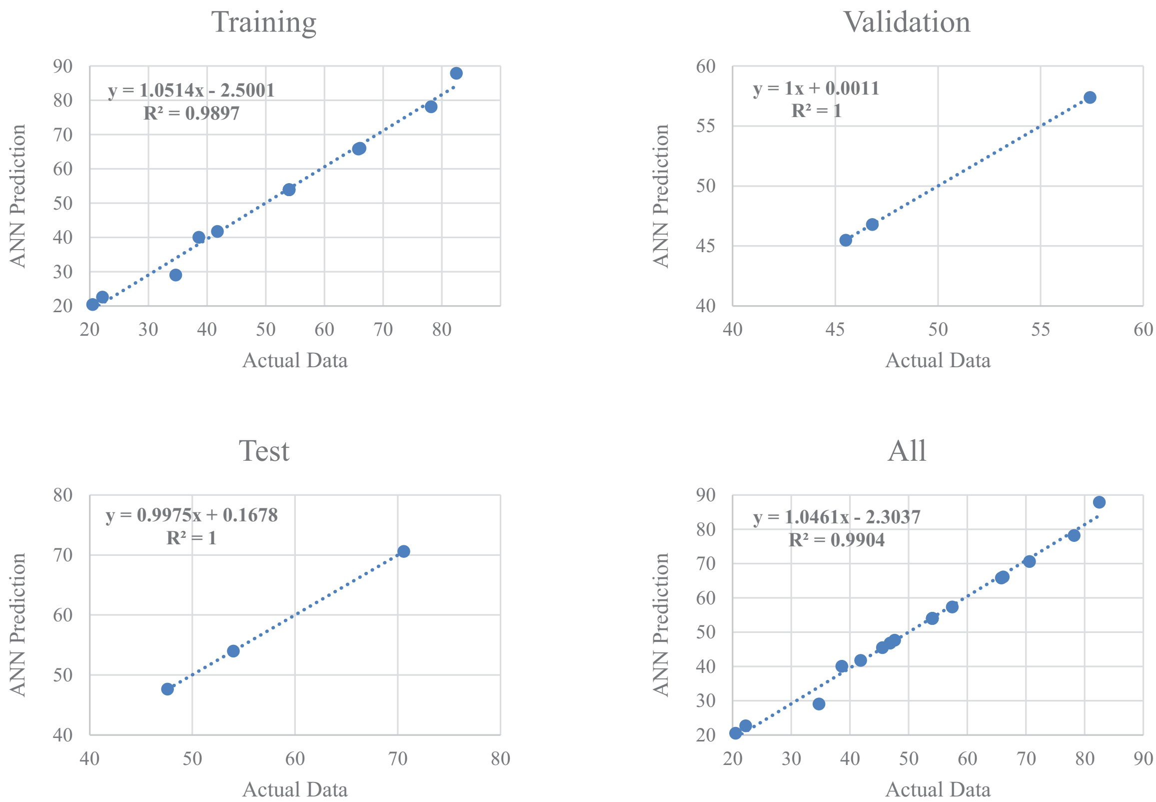

Fig. 11. Scatter plot of the ANN predicted vs. experimental data of MG dye removal by raw pumice.

Table 8
Accuracy assessment of the RSM and ANN models

Factors	1 N		6 N		12 N		Raw pumice	
	RSM	ANN	RSM	ANN	RSM	ANN	RSM	ANN
R^2	0.917	0.957	0.907	0.995	0.882	0.983	0.915	0.990
$R^2_{adj.}$	0.902	0.955	0.889	0.995	0.860	0.982	0.890	0.989
RMSE	4.711	3.795	6.819	1.351	5.810	2.27	4.733	1.761
MAE	4.00	2.996	3.394	0.690	5.215	1.654	4.005	0.688
AAD	6.498	5.192	6.593	0.988	7.801	2.351	8.514	1.521

the pseudo-second-order kinetic model described the experimental data. The absorption coefficient (R_L) and absorbance intensity ($1/n$) for all adsorbed modified forms were in the optimal range of 0–1, which indicated the appropriate adsorbent effect on dye removal.

After that, RSM and ANN were applied to predict the process. The resulting models were statistically analyzed and compared and the predicted values showed that the ANN model is more reliable for predicting this process.

Acknowledgment

The authors gratefully acknowledge the Research Council of Kermanshah University of Medical Sciences (Grant Number: 93049) for financial support.

References

[1] A. Azari, H. Gharibi, B. Kakavandi, G. Ghanizadeh, A. Javid, A.H. Mahvi, K. Sharafi, T. Khosravia, Magnetic adsorption separation process: an alternative method of mercury extracting from aqueous solution using modified chitosan coated Fe_3O_4 nanocomposites, J. Chem. Technol. Biotechnol., 92 (2017) 188–200.

[2] Y. Vasseghian, E.-N. Dragoi, Modeling and optimization of acid blue 193 removal by UV and peroxydisulfate process, J. Environ. Eng., 144 (2018) 06018003.

[3] K. Sharafi, A.M. Mansouri, A.A. Zinatizadeh, M. Pirsaheb, Adsorptive removal of methylene blue from aqueous solutions by pumice powder: process modelling and kinetic evaluation, Environ. Eng. Manage. J. (EEMJ), 14 (2015) 1067–1078.

[4] M. Pirsaheb, Z. Rezai, A. Mansouri, A. Rastegar, A. Alahabadi, A.R. Sani, K. Sharafi, Preparation of the activated carbon from India shrub wood and their application for methylene

blue removal: modelling and optimization, Desal. Wat. Treat., 57 (2016) 5888–5902.
[5] B. Hameed, M. El-Khaiary, Batch removal of malachite green from aqueous solutions by adsorption on oil palm trunk fibre: equilibrium isotherms and kinetic studies, J. Hazard. Mater., 154 (2008) 237–244.
[6] M. Anbia, A. Ghaffari, Removal of malachite green from dye wastewater using mesoporous carbon adsorbent, J. Iran. Chem. Soc., 8 (2011) S67–S76.
[7] A. Karami, K. Karimyan, R. Davoodi, M. Karimaei, K. Sharafie, S. Rahimi, T. Khosravi, M. Miri, H. Sharafi, A. Azari, Application of response surface methodology for statistical analysis, modeling, and optimization of malachite green removal from aqueous solutions by manganese-modified pumice adsorbent, Desal. Wat. Treat., 89 (2017) 150–161.
[8] Y. Uma, U. Sharma, Removal of malachite green from aqueous solutions by adsorption on to timber waste, Int. J. Environ. Eng. Mgmt., 4 (2013) 631–638.
[9] A.S. Sartape, A.M. Mandhare, V.V. Jadhav, P.D. Raut, M.A. Anuse, S.S. Kolekar, Removal of malachite green dye from aqueous solution with adsorption technique using Limonia acidissima (wood apple) shell as low cost adsorbent, Arab. J. Chem., 10 (2017) S3229–S3238.
[10] T. Santhi, S. Manonmani, V. Vasantha, Y. Chang, A new alternative adsorbent for the removal of cationic dyes from aqueous solution, Arab. J. Chem., 9 (2016) S466–S474.
[11] F. Gündüz, B. Bayrak, Biosorption of malachite green from an aqueous solution using pomegranate peel: equilibrium modelling, kinetic and thermodynamic studies, J. Mol. Liq., 243 (2017) 790–798.
[12] M. Moradi, M. Fazlzadehdavil, M. Pirsaheb, Y. Mansouri, T. Khosravi, K. Sharafi, Response surface methodology (RSM) and its application for optimization of ammonium ions removal from aqueous solutions by pumice as a natural and low cost adsorbent, Arch. Environ. Prot., 42 (2016) 33–43.
[13] F.Ö. Akbal, N. Akdemir, A.N. Onar, FT-IR spectroscopic detection of pesticide after sorption onto modified pumice, Talanta, 53 (2000) 131–135.
[14] M. Moradi, A.M. Mansouri, N. Azizi, J. Amini, K. Karimi, K. Sharafi, Adsorptive removal of phenol from aqueous solutions by copper (cu)-modified scoria powder: process modeling and kinetic evaluation, Desal. Wat. Treat., 57 (2016) 11820–11834.
[15] M. Moradi, M. Soltanian, M. Pirsaheb, K. Sharafi, S. Soltanian, A. Mozafari, The Efficiency Study of pumice Powder to Lead Removal from the Aquatic Environment: Isotherms and Kinetics of the Reaction, J. Mazand. Univ. Med. Sci. (JMUMS), 23 (2014) 64–75.
[16] M. Naderi, K. Sharafi, Removal comparison of methylene blue dye by pumice stone and powder activated carbon from aqueous solutions, Int. J. Pharm. Technol., 8 (2016) 10958–10966.
[17] D. Baş, I.H. Boyacı, Modeling and optimization I: Usability of response surface methodology, J. Food Eng., 78 (2007) 836–845.
[18] N. Mirzaei, H.R. Ghaffari, K. Sharafi, A. Velayati, G. Hoseindoost, S. Rezaei, A.H. Mahvi, A. Azari, K. Dindarloo, Modified natural zeolite using ammonium quaternary based material for Acid red 18 removal from aqueous solution, J. Environ. Chem. Eng., 5 (2017) 3151–3160.
[19] M. Pirsaheb, M. Moradi, H. Ghaffari, K. Sharafi, Application of response surface methodology for efficiency analysis of strong non-selective ion exchange resin column (A 400 E) in nitrate removal from groundwater, Int. J. Pharm. Technol., 8 (2016) 11023–11034.
[20] Y. Vasseghian, M. Ahmadi, M. Joshaghani, Simultaneous ash and sulphur removal from bitumen using column flotation technique: experiments, RSM modeling and optimization, Phys. Chem. Res., 5 (2017) 195–204.
[21] M. Moghri, E.N. Dragoi, A. Salehabadi, D.K. Shukla, Y. Vasseghian, Effect of various formulation ingredients on thermal characteristics of PVC/clay nanocomposite foams: experimental and modeling, ePolymers, 17 (2017) 119–128.
[22] M. Pirsaheb, T. Khosravi, M. Fazlzadeh, K. Sharafie, Effects of loading rate, resin height, and bed volume on nitrate removal from drinking water by non-selective strong anion exchange resin (A400E), Desal. Wat. Treat., 89 (2017) 127–135.
[23] C.-C. Huang, H.-S. Li, C.-H. Chen, Effect of surface acidic oxides of activated carbon on adsorption of ammonia, J. Hazard. Mater., 159 (2008) 523–527.
[24] M. Pirsaheb, M. Mohamadi, A.M. Mansouri, A.A. Zinatizadeh, S. Sumathi, K. Sharafi, Process modeling and optimization of biological removal of carbon, nitrogen and phosphorus from hospital wastewater in a continuous feeding & intermittent discharge (CFID) bioreactor, Korean J. Chem. Eng., 32 (2015) 1340–1353.
[25] N. Mansourian, G. Javedan, M. Darvishmotevalli, K. Sharafi, H. Ghaffari, H. Sharafi, H. Arfaeinia, Efficiency evaluation of zeolite powder, as an adsorbent for the removal of nickel and chromium from aqueous solution: isotherm and kinetic study, Int. J. Pharm. Technol., 8 (2016) 13891–13907.
[26] H. Arfaeinia, B. Ramavandi, K. Sharafi, S. Hashemi, Reductive degradation of ciprofloxacin in aqueous using nanoscale zero valent iron modificated by Mg-aminoclay, Int. J. Pharm. Technol., 8 (2016) 13125–13136.
[27] T.W. Weber, R.K. Chakravorti, Pore and solid diffusion models for fixed bed adsorbers, J. Am. Inst. Chimica. Eng., 20 (1974) 228238.
[28] H. Arfaeinia, H. Sharafi, M. Moradi, M. Ehsanifar, S.E. Hashemi, Efficient degradation of 4-chloro- 2-nitrophenol using photocatalytic ozonation with nano-zinc oxide impregnated granular activated carbon (ZnO–GAC), Desal. Wat. Treat., 93 (2017) 145–151.
[29] M. Pirsaheb, H. Mohammadi, K. Sharafi, A. Asadi, Fluoride and nitrate adsorption from water by Fe (III)-doped scoria: optimizing using response surface modeling, kinetic and equilibrium study, Water Sci. Technol. Water Supply, 18 (2018) 1117–1132.
[30] GH. Safari, M. Zarrabi, M. Hoseini, H. Kamani, J. Jaafari, A.H. Mahvi, Trends of natural and acidengineered pumice onto phosphorus ions in aquatic environment: adsorbent preparation, characterization, and kinetic and equilibrium modeling, Desal. Wat. Treat., 54 (2015) 3031–3043.
[31] D. Naghipour, K. Taghavi, J. Jaafari, Y. Mahdavi, M. Ghanbari Ghozikali, R. Ameri, A. Jamshidi, A.H. Mahvi, Statistical modeling and optimization of the phosphorus biosorption by modified Lemna minor from aqueous solution using response surface methodology (RSM), Desal. Wat. Treat., 57 (2016) 19431–19442.
[32] A. Azari, A. Mesdaghinia, G. Ghanizadeh, H. Masoumbeigi, M. Pirsaheb, H.R. Ghafari, T. Khosravi, K. Sharafi, Which is better for optimizing the biosorption process of lead–central composite design or the Taguchi technique?, Water Sci. Technol. Water Supply, 74 (2016) 1446–1456.
[33] M.N. Sepehr, F. Allani, M. Zarrabi, M. Darvishmotevalli, Y. Vasseghian, S. Fadaei, M.M. Fazli, Dataset for adsorptive removal of tetracycline (TC) from aqueous solution via natural light weight expandedclay aggregate (LECA) and LECA coated with manganese oxide nanoparticles in the presence of H_2O_2, Data Brief, 22 (2019) 676–686.
[34] S. Abo-Farha, Comparative study of oxidation of some azo dyes by different advanced oxidation processes: Fenton, Fenton-like, photo-Fenton and photo-Fenton-like, J. Am. Sci., 6 (2010) 128–142.
[35] M. Danish, T. Ahmad, S. Majeed, M. Ahmad, L. Ziyang, Z. Pin, S.S. Iqubal, Use of banana trunk waste as activated carbon in scavenging methylene blue dye: kinetic, thermodynamic, and isotherm studies, Bioresour. Technol. Rep., 3 (2018) 127–137.
[36] A. Esmaeili, E. Hejazi, Y. Vasseghian, Comparison study of biosorption and coagulation/air flotation methods for chromium removal from wastewater: experiments and neural network modeling, RSC Adv., 5 (2015) 91776–91784.
[37] R.R. Kalantary, M. Moradi, M. Pirsaheb, A. Esrafili, A.J. Jafari, M. Gholami, Y. Vasseghian, E. Antolini, E.-N. Dragoi, Enhanced photocatalytic inactivation of E. coli by natural pyrite in presence of citrate and EDTA as effective chelating agents: experimental evaluation and kinetic and ANN models, J. Environ. Chem. Eng., 7 (2019) 102906.

[38] L.P. Lingamdinne, J. Singh, J.-S. Choi, Y.-Y. Chang, J.-K. Yang, R.R. Karri, J.R. Koduru, Multivariate modeling via artificial neural network applied to enhance methylene blue sorption using graphene-like carbon material prepared from edible sugar, J. Mol. Liq., 265 (2018) 416–427.
[39] S.A. Mousavi, Y. Vasseghian, A. Bahadori, Evaluate the performance of Fenton process for the removal of methylene blue from aqueous solution: experimental, neural network modeling and optimization, Environ. Prog. Sustain. Energy, (2018) (in Press), doi: 10.1002/ep.13126.
[40] Y. Vasseghian, N. Heidari, M. Ahmadi, G. Zahedi, A.A. Mohsenipour, Simultaneous ash and sulphur removal from bitumen: experiments and neural network modeling, Fuel. Process. Technol., 125 (2014) 79–85.
[41] O.M. Alharbi, Sorption, kinetic, thermodynamics and artificial neural network modelling of phenol and 3-amino-phenol in water on composite iron nano-adsorbent, J. Mol. Liq., 260 (2018) 261–269.
[42] M.K. Uddin, R.A.K. Rao, K.V.C. Mouli, The artificial neural network and Box-Behnken design for Cu^{2+} removal by the pottery sludge from water samples: equilibrium, kinetic and thermodynamic studies, J. Mol. Liq., 266 (2018) 617–627.
[43] M. Huang, C. Xu, Z. Wu, Y. Huang, J. Lin, J. Wu, Photocatalytic discolorization of methyl orange solution by Pt modified TiO_2 loaded on natural zeolite, Dyes Pigm., 77 (2008) 327–334.
[44] R. Baran, Y. Millot, T. Onfroy, J.-M. Krafft, S. Dzwigaj, Influence of the nitric acid treatment on Al removal, framework composition and acidity of BEA zeolite investigated by XRD, FTIR and NMR, Microporous Mesoporous Mater., 163 (2012) 122–130.
[45] S. Dzwigaj, P. Massiani, A. Davidson, M. Che, Role of Silanol Groups in the Incorporation of V in β Zeolite, J. Mol. Catal. A, 155 (2000) 169–182.
[46] P. Panneerselvam, N. Thinakaran, K. Thiruvenkataravi, M. Palanichamy, S. Sivanesan, Phosphoric acid modified-Y zeolites: A novel, efficient and versatile ion exchanger, J. Hazard. Mater., 159 (2008) 427–434.
[47] M. Heydari, K. Karimyan, M. Darvishmotevalli, A. Karami, Y. Vasseghian, N. Azizi, M. Ghayebzadeh, M. Moradi, Data for efficiency comparison of raw pumice and manganese-modified pumice for removal phenol from aqueous environments—Application of response surface methodology, Data Brief, 20 (2018) 1942–1954.
[48] Y. Kim, C. Kim, I. Choi, S. Rengaraj, J. Yi, Arsenic removal using mesoporous alumina prepared via a templating method, Environ. Sci. Technol., 38 (2004) 924–931.
[49] R. Ajemba, Alteration of bentonite from Ughelli by nitric acid activation: kinetics and physicochemical properties, Indian J. Sci., Technol., 6 (2013) 4076–4083.
[50] J.-X. Guo, S. Shu, X.-L. Liu, X.-J. Wang, H.-Q. Yin, Y.-H. Chu, Influence of Fe loadings on desulfurization performance of activated carbon treated by nitric acid, Environ. Technol., 38 (2017) 266–276.
[51] T.L. Seey, M. Kassim, Acidic and basic dyes removal by adsorption on chemically treated mangrove barks, Int. J. Appl, 2 (2012) 270–276.
[52] L.W. Low, T.T. Teng, A.F. Alkarkhi, A. Ahmad, N. Morad, Optimization of the adsorption conditions for the decolorization and COD reduction of methylene blue aqueous solution using low-cost adsorbent, Water Air Soil Pollut., 214 (2011) 185–195.
[53] B. Hameed, M. El-Khaiary, Malachite green adsorption by rattan sawdust: Isotherm, kinetic and mechanism modeling, J. Hazard. Mater., 159 (2008) 574–579.
[54] K.M. Al-Ahmary, Kinetics and thermodynamic study of Malachite Green adsorption on seeds of dates, Int. J. Sci. Basic Appl., 2 (2013) 27–37.
[55] T. Santhi, S. Manonmani, T. Smitha, Removal of malachite green from aqueous solution by activated carbon prepared from the epicarp of *Ricinus communis* by adsorption, J. Hazard. Mater., 179 (2010) 178–186.
[56] N. Moraci, P.S. Calabrò, Heavy metals removal and hydraulic performance in zero-valent iron/pumice permeable reactive barriers, J. Environ. Manage., 91 (2010) 2336–2341.
[57] A.K. Panda, B.G. Mishra, D.K. Mishra, R.K. Singh, Effect of sulphuric acid treatment on the physico chemical characteristics of kaolin clay, Colloids Surf., A, 363 (2010) 98–104.
[58] F. Akbal, Adsorption of basic dyes from aqueous solution onto pumice powder, J. Colloid Interface Sci., 286 (2005) 455–458.
[59] M. Visa, C. Bogatu, A. Duta, Simultaneous adsorption of dyes and heavy metals from multicomponent solutions using fly ash, AppL. Surf. Sci., 256 (2010) 5486–5491.
[60] M. Doğan, M. Alkan, A. Türkyilmaz, Y. Özdemir, Kinetics and mechanism of removal of methylene blue by adsorption onto perlite, J. Hazard. Mater., 109 (2004) 141–148.
[61] M.A. Al-Ghouti, M.A. Khraisheh, M.N. Ahmad, S. Allen, Adsorption behaviour of methylene blue onto Jordanian diatomite: a kinetic study, J. Hazard. Mater., 165 (2009) 589–598.
[62] M. Moradi, M. Heydari, M. Darvishmotevalli, K. Karimyan, V.K. Gupta, Y. Vasseghian, H. Sharafi, Kinetic and modeling data on phenol removal by Iron-modified Scoria Powder (FSP) from aqueous solutions, Data Brief, 20 (2018) 957–968.
[63] I. Uzun, Kinetics of the adsorption of reactive dyes by chitosan, Dyes Pigm., 70 (2006) 76–83.
[64] K. Sharafi, M. Pirsaheb, V.K. Gupta, S. Agarwal, M. Moradi, Y. Vasseghian, E.-N. Dragoi, Phenol adsorption on scoria stone as adsorbent-Application of response surface method and artificial neural networks, J. Mol. Liq., 274 (2019) 699–714.